

## X-RAY OBSERVATIONS OF GRAVITATIONALLY LENSED QUASARS; EVIDENCE FOR A HIDDEN QUASAR POPULATION

G. CHARTAS<sup>1</sup>*The Astrophysical Journal, in press*

## ABSTRACT

X-ray observations are presented of gravitationally lensed quasars with redshifts ranging between 1 and 4. The large magnification factors of gravitationally lensed (GL) systems allow us to investigate the properties of quasars with X-ray luminosities that are substantially lower than those of unlensed ones and also provide an independent means of estimating the contribution of faint quasars to the hard X-ray component of the cosmic X-ray background. Spectral indices have been estimated in the rest frame energy bands 0.5 - 1keV (soft), 1 - 4keV (mid) and 4 - 20keV (hard). Our spectral analysis indicate a flattening of the spectral index in the hard band for 2 radio-loud quasars in the GL quasar sample for which the data have moderate signal-to-noise ratio. These results are consistent with the reported spectral properties of non-lensed radio-loud quasars, however, there are no indications of spectral hardening towards fainter X-ray fluxes.

We have identified a large fraction of Broad Absorption Line (BAL) quasars amongst the GL quasar population. We find that approximately 35% of radio-quiet GL quasars contain BAL features which is significantly larger than the 10% fraction of BAL quasars presently found in optically selected flux limited quasar samples. We present a simple model that estimates the effects of attenuation and lens magnification on the luminosity function of quasars and that explains the observed fraction of GL BAL quasars. These observations suggest that a large fraction of BAL quasars are missed from flux limited optical surveys.

Modeling of several X-ray observations of the GL BAL quasar PG1115+080 suggests that the observed large X-ray variability may be caused in part by a variable intrinsic absorber consistent with previously observed variability of the BAL troughs in the UV band. The observed large X-ray flux variations in PG1115+080 offer the prospect of considerably reducing errors in determining the time delay with future X-ray monitoring of this system and hence constraining the Hubble constant  $H_0$ .

*Subject headings:* gravitational lensing — quasars: —X-rays: galaxies

## 1. INTRODUCTION

Several attempts have been made to characterize the properties of distant and faint quasars and compare them to those of relatively nearby and bright ones. (Bechtold et al. 1994; Elvis et al. 1994; Vikhlinin et al. 1995; Cappi et al. 1997; Scharrel et al. 1996; Laor et al. 1997; Yuan et al. 1998; Brinkmann et al. 1997; Reeves et al. 1997; Fiore et al. 1998). The evolution of quasar properties is in part studied by identifying changes in spectral properties with redshift. Information obtained from estimating the X-ray properties of quasars as a function of X-ray luminosity and redshift may be useful in constraining physical accretion disk models that explain the observed AGN continuum emission. The study of X-ray properties of quasars with relatively low luminosity may also provide clues to the nature of the

remaining unresolved portion of the hard component of the cosmic X-ray background (XRB) (see, for example, Inoue et al. 1996; Ueda 1996; Ueda et al. 1998).

The Gravitational Lensing (GL) effect has been widely employed as an analysis tool in a variety of astrophysical situations. The study of GL systems (GLS) in the radio and optical community has proven to be extremely rewarding by providing constraints on cosmological parameters  $\Lambda$  and  $H_0$  (Kochanek 1996, Falco et al. 1997), by probing the evolution of mass-to-light ratios of high redshift galaxies (Keeton et al. 1998), by probing the evolution of the interstellar medium of distant galaxies (Nadeau et al. 1991), and by determining the total mass, spatial extent and ionization conditions of intervening absorption sys-

<sup>1</sup>Astronomy and Astrophysics Department, The Pennsylvania State University, University Park, PA 16802.

tems. The study of GL quasars in the X-ray band has been limited until now, the main limiting factor being the collecting area and spectral resolution of current X-ray telescopes combined with the small angular separations of lensed quasar images. One of the main objectives of this paper is to make use of the magnification effect of GL systems to investigate the X-ray properties of faint radio-loud and radio-quiet quasars.

In many cases the available X-ray spectra of distant quasars have relatively low signal-to-noise ratio (S/N). This has led to the development of various techniques to aid the study of faint quasars with 0.2 - 2 keV X-ray fluxes below  $1 \times 10^{-14}$  erg s $^{-1}$  cm $^{-2}$ . Most of these observational and analysis techniques employed to date to study the evolution and spectral emission mechanism of faint quasars are in general a slight variation of two distinct approaches. On the one end we find techniques that are based on summing the individual spectra of many faint X-ray sources taken from a large and complete sample (see for example Schartel et al. 1996; Vikhlinin et al. 1995). The goal of stacking is to obtain a single, high signal-to-noise ratio spectrum that contains enough counts to allow spectral fitting with quasar emission models. In some cases, where the initial sample is large enough, the spectra can be summed into bins of X-ray flux, redshift and radio luminosity class. Schartel et al. 1996 applied the stacking technique to a complete quasar sample and found that the mean spectral index for the stacked radio-quiet quasar spectrum was significantly ( $\sim 2\sigma$ ) steeper than that of the stacked radio-loud quasar spectrum. Several of the assumptions made in this analysis which were related to the general properties of the quasars may, however, strongly influence the further interpretation of the results. It was assumed, for example, that quasar spectra follow single power-laws over rest frame energies ranging between  $(1+z)E_{min}$  and  $(1+z)E_{max}$ , where  $E_{min}$  and  $E_{max}$  are the minimum and maximum energy bounds, respectively, of the bandpass of the X-ray observatory and  $z$  is the redshift of the quasar. Analyzed in the observer's frame, quasar spectra with concave spectral slopes of increasing redshift would appear to be flatter as a consequence of the cosmological redshift. Any implications of evolutionary change within the quasar spectrum derived from the analysis of stacked spectra in observed frames would need to include the effect of cosmological redshift. Detailed spectra of quasars however indicate in general the presence of several components each associated to a different physical process. For example, several known processes contributing to the observed X-ray spectra are Compton reflection of photons in the disk coronae by the disk which becomes significant at rest

energies above  $\sim 10$ keV, inverse Compton scattering of photons in the disk coronae by UV photons originating from the disk resulting in a boost of photon energies from the UV range into the soft X-ray range (this is the mechanism that produces the observed power-law spectrum in the 2-10keV range), accretion disk emission, absorption by highly ionized gas (warm absorbers), beamed X-ray emission from jets which may be a large contributor for distant radio-loud quasars, absorption by accretion disk winds, and intervening absorption by damped Lyman alpha systems. The stacked spectrum therefore contains contributions from quasars of different redshifts and possibly spectral shapes that make the interpretation of the results difficult.

Vikhlinin et al. 1995, using the ROSAT EMSS sample of 2678 sources, produced stacked spectra within several flux bins. They find a significant continuous flattening of the fitted spectral slopes from higher towards lower X-ray fluxes. One interesting result of their study is that the spectral slope at the very faint end is approximately equal to the slope of the hard (2 - 10keV) X-ray background. The unknown nature of many of the point sources included in the Vikhlinin sample, the inclusion of sources with different redshifts and the calculation of observed rest spectral indices complicates the interpretation of the results.

A second technique used to study the general properties of quasars is based on obtaining deep X-ray observations of a few quasars. One advantage of such an approach is that the properties of individual quasars are not smeared out as with stacking methods. The faint fluxes however require extremely long observing times to achieve useable S/N. When total counts are low the quasar X-ray spectra are commonly characterized by a hardness ratio defined as  $R = (H - S)/(H + S)$ , where  $H$  and  $S$  are the number of counts within some defined hard and soft energy band in the observer's frame respectively.

In this paper we outline an alternative approach to investigating the emission mechanism of radio-loud and quiet quasars at high redshift. The gravitational lensing magnification of distant quasars allows us to investigate the X-ray properties of quasars with luminosities relatively lower than those of unlensed quasars of similar redshifts. The amplification factors produced by lensing depends on the geometry of the lensing system and for our sample range between 2 and 30. The moderate-S/N spectra of our sample allow us to employ spectral models with multiple power-law slopes and perform fits in rest-frame energy bands. Our analysis makes use of the GL amplification effect to extend the study of quasar properties to unlensed X-ray flux levels as low as a few  $\times 10^{-16}$  erg s $^{-1}$  cm $^{-2}$ . The limiting sensitivity of

the ROSAT All-Sky Survey, for example, on which many recent studies are based is a few  $\times 10^{-13}$  erg s $^{-1}$  cm $^{-2}$ .

For a GL system with a lens that can be modeled well with a singular isothermal sphere (SIS) model the amplification is straightforward to derive analytically. In most observed cases, however, the deflector is a galaxy or cluster of galaxies with a gravitational potential that does not follow the SIS model and more sophisticated potential models need to be invoked to successfully model these GL systems. To estimate the intrinsic X-ray luminosity of GL quasars in our sample we have incorporated magnification factors determined from modeling of the GL systems with a variety of lens potentials.

We performed fits of spectral models to the X-ray data in three rest energy bins, soft from 0.5 - 1 keV, mid from 1 - 4 keV, and high from 4 - 20 keV. Working in the quasar rest frame as opposed to the observers rest frame allows us to distinguish between true spectral evolution of quasars with redshift and apparent change in quasar spectra due to the cosmological redshift of quasar spectra through a fixed energy window in the observer's rest frame.

Our search of the ROSAT and ASCA archives yielded 16 GL systems detected in X-rays out of a total of approximately 40 GL candidates. Six of the GL quasars have observed X-ray spectra of medium-S/N. Our search for X-ray counterparts to known GL quasars resulted in the identification of the relatively X-ray bright radio-quiet quasar SBS0909+532 with an estimated 0.2-2 keV flux of about  $7 \times 10^{-13}$  erg s $^{-1}$  cm $^{-2}$ . Another interesting result of our search was the identification of a relatively large fraction of radio-quiet GL quasars with BAL quasars. In particular we find that at least 35% of the known radio-quiet GL quasars are BAL quasars. This value is significantly larger than the  $\sim 10\%$  value presently quoted from optical surveys.

In section 2 we present details of X-ray observations of GL quasars and describe the analysis techniques used to extract and fit the X-ray spectra. Estimates of the flux magnification factors and unlensed luminosities for the GL systems studied in this paper are presented in section 3. A description of the properties of each GL quasar is presented in section 4. Included in this section are results from spectral modeling of several X-ray observations of the variable GL BAL quasar PG1115+080. Finally, in section 5 we summarize the spectral properties of faint quasars as implied by spectral fits to a sample of GL quasar spectra and provide a plausible explanation for the apparently large fraction of GL BAL quasars that we observe.

## 2. X-RAY OBSERVATIONS AND DATA ANALYSIS

The X-ray observations presented here were performed with the ROSAT and ASCA observatories. Results for the spectral analyses in the X-ray band for the GL quasars Q0957+561, HE1104-1805, PKS1830-211 and Q1413+117 have already been published (Chartas et al. 1995, 1998; Reimers et al. 1995; Mathur et al. 1997; Green & Mathur, 1996) while results from X-ray spectral analyses for the quasars SBS0909+532, B1422+231, PG1115+080, 1208+1011 and QJ0240-343 are presented here for the first time. We have included in Table 1 several additional GL systems observed in the X-ray band. These observations however yielded either very low-S/N detections or were made with the ROSAT HRI which provides very limited spectral information. X-ray spectra of the GL quasars Q0957+561, 1422+231, HE1104-1805, SBS0909+532 and PG1115+080 with best fit models are presented in Figure 1 through Figure 5 respectively.

The wide separation quasar pairs MG 0023+171, Q1120+0195, LBQS 1429-008 and QJ0240-343 are considered problematic GL candidates that may be binary quasars and not gravitational lenses (Kochanek et al. 1999). However, recent STIS spectroscopy of Q1120+0195(UM425) has revealed broad absorption line features in both lensed images thus confirming the lens nature of this wide separation system (Smette et al. 1998). The origin of the detected X-ray emission for the GL systems RXJ0921+4528 and RXJ0911.4+0551 cannot be determined from the presently available poor S/N ASCA GIS and ROSAT HRI observations respectively. The most likely origins are either the lensed quasar and/or a possible lensing cluster. In Table 1 we list the ASCA and ROSAT observations of GL quasars with detected X-rays.

The spatial resolution for on axis pointing of the ROSAT HRI, ROSAT PSPC and ASCA GIS is about 5'', 25'' and 3' respectively. Thus only for the ROSAT HRI observation of Q0957+561 was it possible to resolve the lensed X-ray images (Chartas et al. 1995).

For the data reduction of the ASCA and ROSAT observations we used the FTOOLS package XSELECT. The ASCA SIS data used in this study were all taken in BRIGHT mode and high, medium and low bit rate data were included in the analysis. We created response matrices and ancillary files for each chip using the FTOOLS tasks `sisrmf` and `ascaarf` respectively. For the ROSAT PSPC data reduction we used the response matrix `pspcb_gain2_256.rmf` supplied by the ROSAT GOF and created ancillary files using the FTOOLS task `pcarf`. Net events shown in Table 1 are corrected for background, vignetting, exposure and point spread function effects

TABLE 1  
ROSAT and ASCA Observations of Gravitationally Lensed Quasars

Object	Observation Date	Instrument	Observation File name Id	Exposure	Net Events <sup>a</sup>	$\Delta\theta^b$	$z_s^c$	$z_l^d$
				<i>s</i>		<i>"</i>		
QJ0240-343	1992 Jan 31	ROSAT PSPC	rp600003n00	10685	30 ± 7	6.1	1.41	
MG0414+0534	1992 Sep 7	ROSAT PSPC	rp200978	4417	58 ± 15	2.1	2.64	0.96
SBS 0909+532	1992 Oct 27	ROSAT PSPC	rp201127n00	3124	179 ± 18	1.11	1.38	
SBS 0909+532	1992 April 28	ROSAT PSPC	rp200561n00	8588	546 ± 39			
SBS 0909+532	1991 April 17	ROSAT PSPC	rp200023n00	1051	94 ± 15			
RXJ0911+0551	<sup>e</sup>	ROSAT HRI	rh704056	<sup>e</sup>	<sup>e</sup>	3.1	2.80	
0921+4528	1994 Apr 16	ASCA GIS	ad71042000	11960	105 ± 32(GIS2)	6.5	1.40	0.4
				11960	86 ± 28(GIS3)			
0921+4528	1993 Oct 27	ROSAT PSPC	rp701398n00	3364	44 ± 21			
0921+4528	1992 May 3	ROSAT PSPC	rp700539n00	4349	30 ± 8			
Q0957+561	1993 Nov 8	ROSAT PSPC	rp701401n00	4472	488 ± 36	6.1	1.41	0.36
Q0957+561	1993 May 9	ASCA GIS	ad60000000	29071	486 ± 92(GIS2)			
				29071	390 ± 70(GIS3)			
Q0957+561	1991 Nov 15	ROSAT PSPC	rp300319	19006	2860 ± 67			
HE1104-1805	1996 May 31	ASCA SIS	ad74069000	35989	2131 ± 89(SIS0)	3.0	2.32	1.66
				35597	1433 ± 64(SIS1)			
HE1104-1805	1993 June 15	ROSAT PSPC	rp180019n00	13493	1282 ± 58			
PG1115+080	1993 Jun 10	ROSAT HRI	rh700890n00	24834	128 ± 14	2.2	1.72	0.31
PG1115+080	1991 Nov 21	ROSAT PSPC	rp700358n00	14221	65 ± 11			
PG1115+080	1979 Dec 5	Einstein IPC	ii1115n08	1585	49 ± 10			
1120+019	1994 May 27	ROSAT HRI	rh701295n00	17746	10 ± 5	6.5	1.47	0.6
1208+1011	1992 June 3	ROSAT PSPC	rp700079a01	2999	16 ± 5	0.48	3.80	1.13
1208+1011	1991 Dec 16	ROSAT PSPC	rp700079a00	2786	9 ± 4			
Q1413+117	1991 July 20	ROSAT PSPC	rp700122n00	27863	43 ± 12	1.2	2.55	
B 1422+231	1995 July 17	ASCA SIS	ad73078010	12921	503 ± 49(SIS0)	1.3	3.62	0.65
				12159	295 ± 35(SIS1)			
B 1422+231	1995 Jan 14	ASCA SIS	ad73078000	21465	906 ± 55(SIS0)			
				21588	850 ± 64(SIS1)			
PKS1830-211	1993 Sept 15	ROSAT PSPC	wp701519n00	17658	1391 ± 47	1.0	2.51	0.89

NOTES-

<sup>a</sup> Net events are corrected for background, vignetting, exposure and point spread function effects using the software tool *SOSTA*. <sup>b</sup>  $\Delta\theta$  is the angular separation of the images. <sup>c</sup>  $z_s$  is the source redshift. <sup>d</sup>  $z_l$  is the lens redshift. <sup>e</sup> RXJ0911+0551 was observed during the ROSAT ALL-Sky Survey (RASS). Bade et al. (1997) quote a HRI countrate of 0.02 cts s<sup>-1</sup>.

using the source analysis tool *SOSTA* (part of the software package XIMAGE).

For the spectral analyses we are mostly limited by the energy resolution and counting statistics to fitting simple absorbed power-law models to the data. In addition to spectral fits in the quasar rest frame we also performed spectral fits in the observer's reference frame to facilitate the comparison of our results to those of previous studies. In Table 2 we show the results from fits of absorbed power-law models within three quasar rest frame energy intervals. In most cases no data are available in the soft interval since the corresponding observed energy interval is redshifted below the low energy quantum efficiency cutoff of the ROSAT XRT/PSPC.

To estimate any significant difference of the spectral properties of our GL sample from those of unlensed quasar samples we computed the merit function,  $\frac{\chi^2}{N}$ , defined by the expression,

$$\frac{\chi^2}{N} = \sum_{i=0}^N \frac{[\alpha_{\nu, GL}(i) - \alpha_{\nu, UL}(i)]^2}{\sigma_{UL}^2(i)} \quad (1)$$

where  $\alpha_{\nu, GL}(i)$  and  $\alpha_{\nu, UL}(i)$  are the spectral indices of the GL and unlensed quasar sample respectively,  $\sigma_{UL}(i)$  are the errors of the spectral indices of the unlensed samples and N is the number of spectral indices compared. We computed the merit function between our data set and that of Fiore et al. 1998. For the comparison we computed the spectral indices  $\alpha_S(0.1 - 0.8 \text{ keV})$  and  $\alpha_H(0.4 - 2.4 \text{ keV})$  in the quasar observed frames. Incorporating the  $1\sigma$  uncertainties in the fitted values for the GL spectral indices we obtain a distribution of values for the merit function with a most likely value of  $\frac{\chi^2}{N} \sim 0.5$  with  $N = 7$ . We therefore conclude that there is no significant difference at the  $\Delta\alpha_{\nu} = 0.3$  level between our lensed sample and the Fiore et al. 1998 sample.

Spectral modeling of the radio-loud and (non-BAL) radio-quiet quasars of our GL sample that have un-

TABLE 2  
Spectral Indices of GL Quasars

Object	$\alpha_\nu$ Soft [0.5 - 1keV] <sup>a</sup>	$\alpha_\nu$ Mid [1 - 4keV] <sup>a</sup>	$\alpha_\nu$ High [4 - 20keV] <sup>a</sup>
Q0957+561	$1.70^{+0.26}_{-0.23}$	$2.41^{+0.08}_{-0.09}$	$1.46^{+0.14}_{-0.15}$
B 1422+231		$2.02^{+0.46}_{-0.53}$	$1.66^{+0.13}_{-0.12}$
PKS1830-211		$-0.2^{+2.7}_{-0.9}$	$1.4^{+1.6}_{-1.3}$
SBS 0909+532	$1.62^{+1.0}_{-0.64}$	$2.25^{+0.74}_{-0.78}$	
HE1104-1805		$1.93^{+0.27}_{-0.28}$	$2.01^{+0.1}_{-0.1}$
RXJ0921+4528 <sup>b</sup>		$1.7^{+2.5}_{-1.3}$	$1.3^{+1.3}_{-0.9}$
PG1115+080		$1.8^{+0.9}_{-0.9}$	
Q1413+117 <sup>c</sup>		$0.5^{+1.2}_{-2.0}$	

NOTES-

Errors quoted on spectral indices are at the 68.3% confidence level.

<sup>a</sup> Quasar rest frame energy band.

<sup>b</sup> Analysis is based on the ASCA GIS2 + GIS3 spectra of April, 16 1994.

<sup>c</sup> The poor S/N PSPC spectrum of Q1413+117 is fitted with a power-law that includes absorption fixed at the Galactic value of  $1.78 \times 10^{20} \text{ cm}^{-2}$

TABLE 3  
Observed X-ray Fluxes and Unlensed Luminosities of Gravitationally Lensed Quasars

Object	$b_{SIE}$ "	e	PA degrees	M	Flux <sup>a</sup> $10^{-13} \text{ erg s}^{-1} \text{ cm}^{-2}$	Luminosity <sup>b</sup> $10^{45} \text{ erg s}^{-1}$
Q0957+561 <sup>c</sup>	3.09	0.64	69	2.5	$2.0^{+0.7}_{-0.6}$	$3.3^{+0.7}_{-0.6}$
HE1104-1805 <sup>d</sup>	1.441	0.414	22.8	10.4	$9.4^{+1.4}_{-1.5}$	$8.2^{+0.7}_{-0.7}$
B1422+231 <sup>e</sup>	0.65	0.63	-53.2	9.8	$17.4^{+2.5}_{-2.7}$	$36^{+5}_{-4}$
PG1115+080 <sup>f</sup>	1.08	0.48	66.7	26.6	$0.54^{+0.05}_{-0.08}$	$0.1^{+0.01}_{-0.01}$
SBS0909+532 <sup>g</sup>				15	$3.13^{+0.9}_{-0.8}$	$0.6^{+0.1}_{-0.1}$
Q1413+117 <sup>h</sup>	0.5	0.48	21.6	9.9	$0.31^{+0.39}_{-0.17}$	$0.4^{+0.25}_{-0.15}$
1208+1011 <sup>i</sup>				22	$0.1^{+0.3}_{-0.1}$	$0.7^{+0.8}_{-0.1}$
MG0414+0534 <sup>j</sup>	1.14	0.38	79.1	27.7	$2.7^{+1.5}_{-0.6}$	$1.8^{+0.1}_{-0.1}$

NOTES-

The X-ray spectra of the non-BAL quasars are fitted over the observed X-ray band with models consisting of simple power-laws with Galactic absorption. The spectra of the two BAL quasars, PG1115+080 and Q1413+117, contain in addition, intrinsic absorption at the redshift of the quasar.

<sup>a</sup> Observed (lensed) 2-10keV flux.

<sup>b</sup> Ratio of the lensed 2-10keV luminosity to the magnification ratio. We used  $H_0 = 50 \text{ km s}^{-1} \text{ Mpc}^{-1}$  and  $q_0 = 0$ .

<sup>c</sup> Estimated flux and luminosity are for the Nov 8 1993 ROSAT PSPC observation of Q0957+561

<sup>d</sup> Estimated flux and luminosity are for the May 1996 ASCA SIS0 observation of HE1104-1805 (fit 1 Table 6)

<sup>e</sup> Estimated flux and luminosity are for the Jan 14 1995 ASCA SIS0 observation of B1422+231 (fit 2 Table 5)

<sup>f</sup> Estimated flux and luminosity are for the Nov 21 1991 ROSAT PSPC observation of PG1115+080 (fit 4 Table 8)

<sup>g</sup> Estimated flux and luminosity are for the Oct 27 1992 ROSAT PSPC observation of SBS0909+532 (fit 1 Table 4)

<sup>h</sup> Estimated flux and luminosity are for the ROSAT PSPC observation of Q1413+117. Due to the poor S/N spectrum of Q1413+117 the flux and luminosity values were estimated assuming a photon index of 2.3 and the error bars reflect the variation of these values for photon indices ranging between 2 and 2.6

<sup>i</sup> Estimated flux and luminosity are for the Dec 16 1991 and June 3 1992 ROSAT PSPC observations of 1208+1011

<sup>j</sup> Estimated flux and luminosity are for the Sep 7 1992 ROSAT PSPC observations of MG0414+0534

lensed X-ray fluxes ranging between  $3 \times 10^{-16}$  and  $1 \times 10^{-12} \text{ erg s}^{-1} \text{ cm}^{-2}$  have indices that are consistent with those of brighter quasars (see Figure 7). In spite of the fact that most of the quasars in our sample have intervening absorption systems (see comments on individual systems) we find that the estimated

photon indices for the very faint non-BAL quasars of our sample do not approach the level of 1.4 of the hard X-ray background.

In Figure 8 we also show that the photon indices of our GL quasar sample do not show any signs of hardening over a range of three orders of magnitude

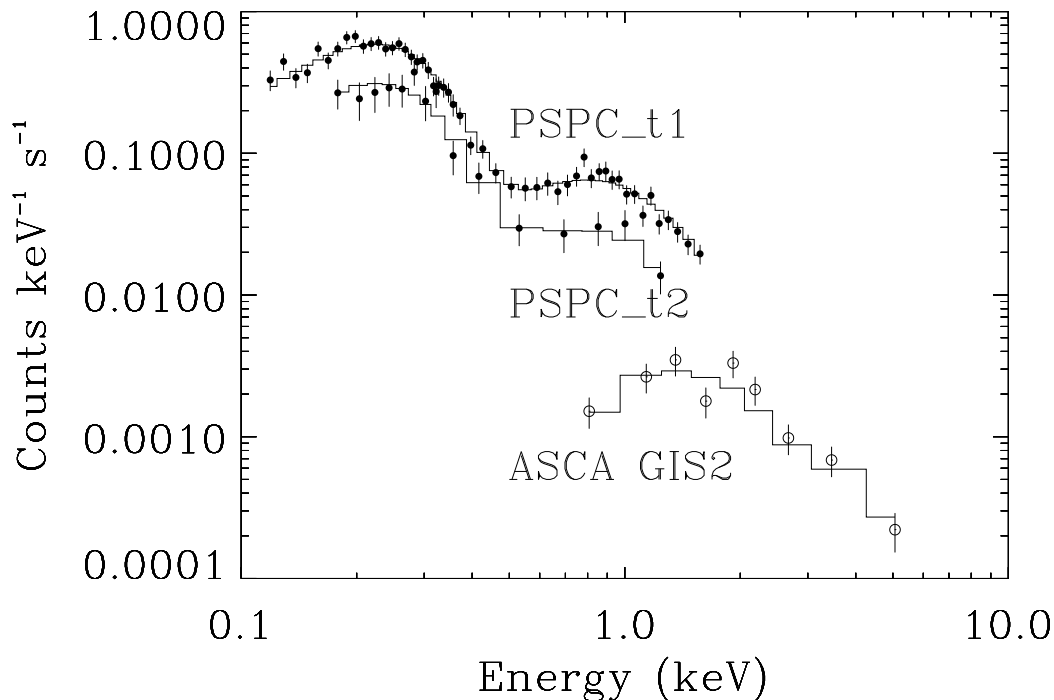


FIG. 1.— ROSAT PSPC and ASCA GIS spectra of Q0957+561 with best fit models.

in unlensed 2-10keV luminosity. The three apparently harder spectra of Figure 7 and Figure 8 correspond to two BAL quasars and one absorbed blazar of our sample. The X-ray spectra of BAL quasars that are modeled as power-laws with Galactic absorption and no intrinsic absorption will erroneously imply relatively low photon indices. For example, spectral fits of a simple power-law plus Galactic absorption model to the X-ray spectrum of PG1115+080 (Fit 1, Table 8) yields a relatively low photon index of 1.4. The presently available spectra of the two BAL quasars of our sample have poor S/N and can not provide significant constraints on the intrinsic absorber column densities.

### 3. QUASAR UNLENSED LUMINOSITY

The apparent surface brightness of gravitationally lensed images is a conserved quantity, however the observed X-ray flux is amplified due to the geometric distortion of the GL images. The lensed quasar images of our sample are not spatially resolved so we only observe the total magnification of the X-ray flux and not the spatial distortion of the image. Gravitational lensing is in general an achromatic effect, however possible differential absorption in the multiple images, microlensing from stars in the lens galaxy and source spectral variability combined with the ex-

pected time delay between photon arrival for each image may produce distinct features in the multiply lensed spectrum of the quasar.

We estimated the unlensed X-ray luminosity of the quasars in our sample by scaling the lensed luminosity determined from the spectral fits to the GL magnification factors. The magnification parameters were derived from fits of singular isothermal ellipsoid SIE lens models (Keeton, Kochanek, & Falco, 1997) to optical and radio observables (e.g. image and lens positions and flux ratios) and incorporating the best fit parameters to derive the convergence,  $\kappa$ , of the lens.

For a SIE lens the convergence  $\kappa(\mathbf{x})$  is given by,

$$\kappa(\mathbf{x}) = \frac{b}{x\sqrt{1 + e \cos(2(\theta - \theta_0))}} \quad (2)$$

where  $b$  is the best-fit critical radius,  $x$  is the distance from the lens galaxy center,  $\theta$  is the position angle of point  $\mathbf{x}$  with respect to the lens galaxy,  $e$  is the ellipticity parameter of the lens and  $\theta_0$  is the major axis position angle.

The magnification  $\mu(x)$  of each lensed image for an SIE lens is given by (Kormann, Schneider, and Bartelmann, 1994),

$$\mu(x) = \frac{1}{(1 - 2\kappa)} \quad (3)$$

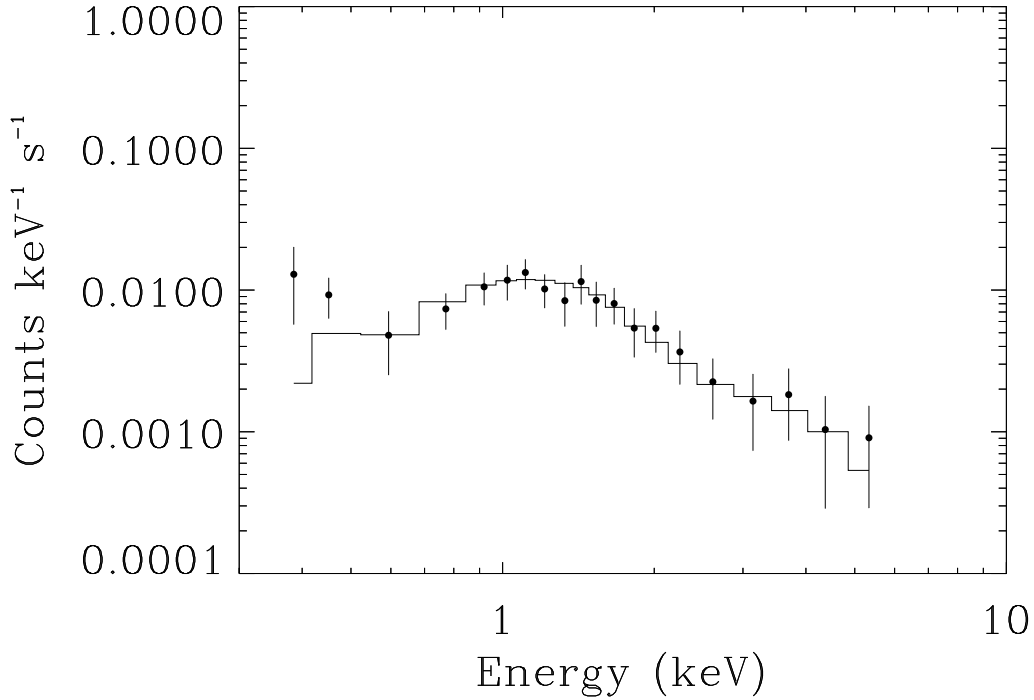


FIG. 2.— ASCA SIS spectrum of 1422+231 with best fit models.

In Table 3 we provide GL model parameters and magnification factors for several GL systems.

#### 4. COMMENTS ON INDIVIDUAL SOURCES

##### 4.1. *The Newly Identified GL X-Ray Source SBS 0909+532*

The radio-quiet quasar SBS0909+532 was recently identified as a candidate gravitational lens system with a source redshift of 1.377, and an image separation of  $1.107''$ . The lens has not yet been clearly identified, however, GL statistics place the most likely redshift for the lens galaxy at  $z_l \simeq 0.5$  with 90% confidence bounds of  $0.18 < z_l < 0.83$  (Kochanek et al. 1997). Optical spectroscopy (Kochanek et al. 1997; Oscoz et al. 1997) has identified heavy element absorption lines of CIII, FeII and Mg II at  $z = 0.83$ . The optical data at this point cannot clearly discern whether the heavy-element absorber is associated with the lensing galaxy.

We searched the HEASARC archive and found a bright X-ray source within  $7''$  of the optical location of SBS0909+532, well within the error bars of the ROSAT pointing accuracy of  $\sim 30''$ . The position of the X-ray counterpart as determined using the *detect* routine, which is part of the XIMAGE software package, is 09h 13m 1.7s,  $52^\circ 59' 39.5''$  (J2000), whereas the optical source coordinates of SBS0909+532 are

09h 13m 2.4s,  $52^\circ 59' 36.4''$  (J2000).

This X-ray counterpart was observed serendipitously with the ROSAT PSPC on April 17 1991, April 28 1992 and October 27 1992 with detected count rates of  $0.057 \pm 0.006$ ,  $0.064 \pm 0.005$  and  $0.09 \pm 0.01$  cts  $s^{-1}$  respectively.

We performed simultaneous spectral fits in the observer frame to the three ROSAT PSPC observations. The results are summarized in Table 4. We considered two types of spectral models. In fit 1 of Table 4 we incorporated a redshifted power-law plus Galactic absorption and in fit 2 we included additional absorption at a redshift of 0.83 (possible lens redshift). Fits 1 and 2 yield acceptable reduced  $\chi^2(\text{dof})$  of 1.00(32) and 1.02(31) respectively. We can rule out absorption columns at  $z = 0.83$  of more than  $7.5 \times 10^{20} \text{ cm}^{-2}$  at the 68.3% confidence level.

We also performed spectral fits in the quasar rest frame bands 0.5 - 1keV (soft band) and 1 - 4 keV (mid band). Simple spectral fits with an absorbed power-law assuming Galactic absorption of  $1.72 \times 10^{20} \text{ cm}^{-2}$  result in spectral indices of  $1.62^{+1.0}_{-0.64}$  and  $2.25^{+0.74}_{-0.78}$  for the soft and mid bands respectively. All errors quoted in this paper are at the 68.3% confidence level unless mentioned otherwise. No X-ray data are presently available for the high energy band 4 - 20 keV. The ROSAT PSPC can only detect pho-

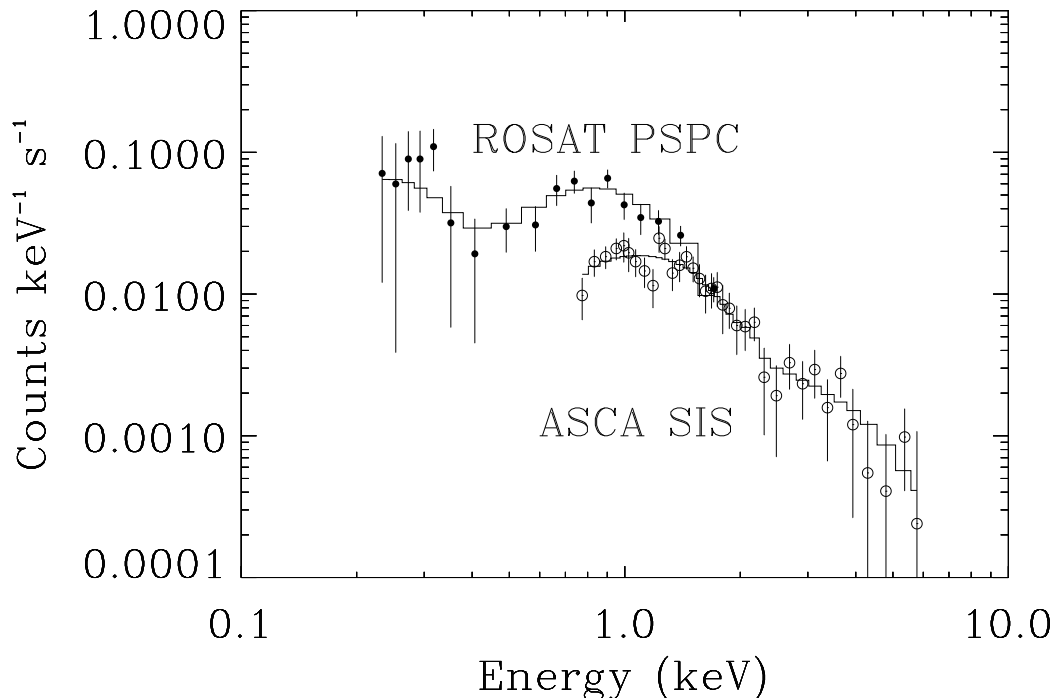


FIG. 3.— ROSAT PSPC and ASCA SIS spectra of HE1104-1805 with best fit models.

tons with energies up to about 3 keV in the rest frame of SBS0909+532. In Figure 4 we show the ROSAT PSPC spectrum of SBS0909+532 together with the best fit absorbed power-law model.

#### 4.2. B1422+231

B1422+231 is a well studied quadrupole GLS with the lensed source being a radio-loud quasar at a redshift of 3.62 (Patnaik et al. 1992) and the lens consisting of a group of galaxies at a redshift of about 0.34 (Tonry, 1998). CIV doublets were found at redshifts of 3.091, 3.382, 3.536 and 3.538 (Bechtold et al. 1995). Strong Mg II and Mg I absorption lines at  $z = 0.647$  have been identified in the quasar spectrum (Angonin - Willaime et al. 1993).

X-ray observations of B1422+231 were made on Jan 14, 1995 for about 21.5ks and July 17, 1995 for about 13 ks with the ASCA satellite. The spectra were extracted from circular regions of  $2.5'$  in radius centered on B1422+231 and the backgrounds were estimated from similar sized circular regions located on a source-free region on the second CCD.

We first modeled the spectra of the two observations separately. Spectral fits in the observer's frame, incorporating power-law models and absorption due to Galactic cold material, yield photon indices of  $1.55^{+0.08}_{-0.08}$  and  $1.46^{+0.1}_{-0.1}$  for the Jan 1995 and July 1995

observations respectively. We searched for possible departures from single power-law models by considering broken power-law models with a break energy fixed at 4 keV (rest frame). The Jan 14, 1995 data are suggestive of spectral flattening at higher energies while the poor S/N of the July 1995 spectrum cannot significantly constrain the spectral slopes.

The 2-10keV X-ray fluxes for the Jan 14, 1995 and July 17, 1995 observations of B1422+231 are estimated to be  $1.70^{+0.46}_{-0.37}$  and  $1.93^{+0.40}_{-0.35} \times 10^{-12}$  erg s $^{-1}$  cm $^{-2}$  respectively (fits 1 and 4 in Table 5).

Spectral fits in the quasar mid and high rest-frame bands for the Jan 14, 1995 observation with absorbed power-law models and assuming Galactic absorption of  $2.52 \times 10^{20}$  cm $^{-2}$  yielded spectral indices of  $2.02^{+0.46}_{-0.53}$  and  $1.66^{+0.13}_{-0.12}$  respectively.

#### 4.3. HE1104-1805

HE1104-1805 is a GL radio-quiet high redshift ( $z=2.316$ ) quasar with an intervening damped Ly $\alpha$  system and a metal absorption system at  $z = 1.66$  and a Mg II absorption system at  $z = 1.32$ . Recent deep near IR imaging of HE1104-1805 (Courbin, Lidman, & Magain, 1998) detect the lensing galaxy at a redshift of 1.66 thus confirming the lens nature of this system.

HE1104-1805 was observed with the ROSAT satel-



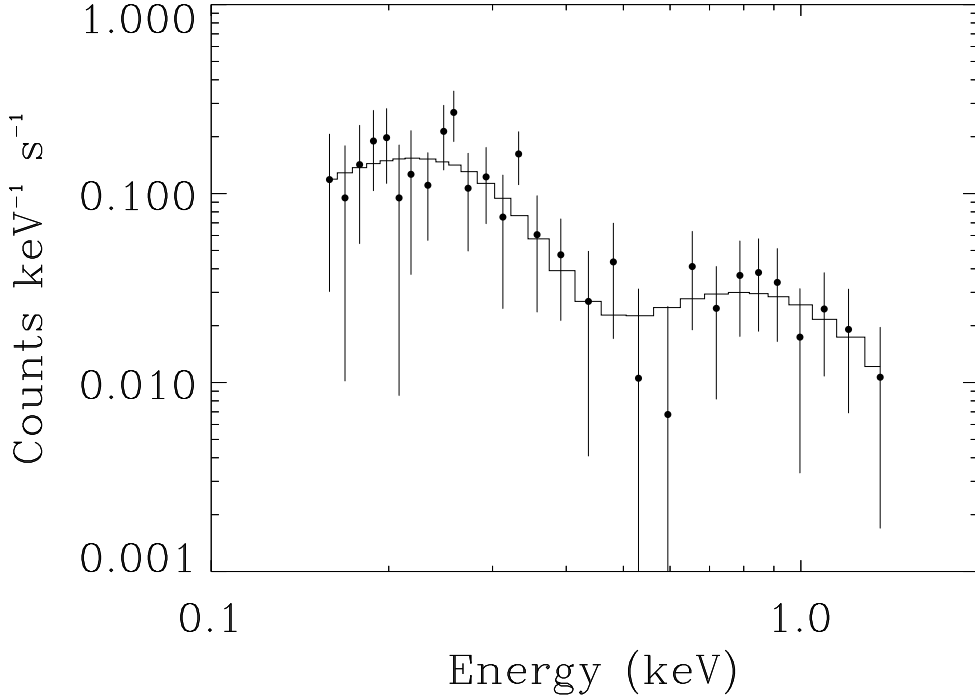


FIG. 4.— ROSAT PSPC spectrum of SBS0909+532 with best fit model.

TABLE 4  
Model Parameters Determined from Spectral Fits to the  
ROSAT PSPC Spectra of SBS0909+532

Fit <sup>a</sup>	Observation <sup>b</sup>	$\alpha_\nu$	$N_H(z=0)$ $10^{22} \text{ cm}^{-2}$	$N_H(z=0.83)$ $10^{22} \text{ cm}^{-2}$	Flux 0.2-2keV $10^{-13} \text{ erg s}^{-1} \text{ cm}^{-2}$	$\chi^2/(dof)$
1	t1+	$2.32^{+0.11}_{-0.11}$	0.017(fixed)	0	$7.19^{+0.35}_{-0.31}$	1.00(32)
	t2+				$5.10^{+0.25}_{-0.22}$	
	t3				$6.48^{+0.31}_{-0.28}$	
2	t1+	$2.56^{+0.43}_{-0.32}$	0.017(fixed)	$0.026^{+0.049}_{-0.026}$	$7.28^{+0.90}_{-1.09}$	1.02(31)
	t2+				$5.12^{+0.63}_{-0.77}$	
	t3				$6.47^{+0.80}_{-0.97}$	

## NOTES-

<sup>a</sup> Fit 1 incorporates a redshifted power-law plus absorption due to cold material at solar abundances fixed to the Galactic value. Fit 2 incorporates a redshifted power-law, absorption due to cold material at solar abundances fixed to the Galactic value and absorption due to cold material at solar abundances located at a  $z=0.83$ . <sup>b</sup> t1, t2 and t3 correspond to the observation dates of April 17 1991, April 28 1992 and October 27 1992 respectively.

lite on June 15 1993 for 13100 sec and with the ASCA satellite on May 31 1996 for 35989 sec with SIS0 and 35597 sec with SIS1. Reimers et al. (1995) have fit the ROSAT spectrum of HE1104-1805 in the 0.2 - 2 keV range with an absorbed power law model and find a photon index of  $2.24 \pm 0.16$ , consistent with our fitted value of  $2.05 \pm 0.2$ . The main difference between the Reimers et al. and Chartas 1999 models, used for

the fits to the ROSAT spectrum of HE1104-1805, is that the former model allows the column density to be a free parameter in the spectral fit while in the latter model the column density is frozen to the Galactic value of  $0.045 \times 10^{22} \text{ cm}^{-2}$ . For the data reduction of the ASCA SIS0 and SIS1 observations we extracted grade 0234 events within circular regions centered on HE1104-1805 and with radii of  $3.2'$ . The background

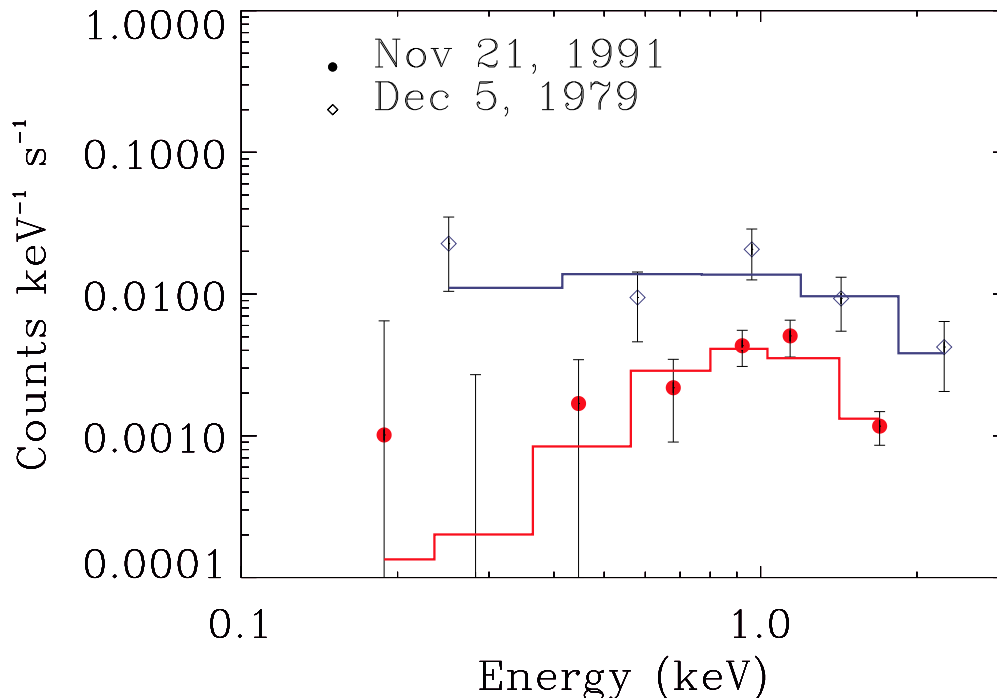


FIG. 5.— Einstein IPC and ROSAT PSPC spectra of PG1115+080 observed on Dec 5, 1979 and Nov 21, 1991 respectively, accompanied by best fit models.

was estimated by extracting events within circular regions in source free areas. High, medium and low bit rate data were combined and only Bright mode data were used in the analysis. We performed several spectral fits to the extracted ASCA spectrum with results summarized in Table 6. A simple spectral fit in the observers frame with an absorbed power-law model yields an acceptable fit with a photon index of  $1.91^{+0.06}_{-0.06}$  and a 2-10 keV flux of about  $9.4^{+1.5}_{-1.4} \times 10^{-13} \text{ erg s}^{-1} \text{ cm}^{-2}$ . In Figure 3 we show the fit of this model to the ASCA data.

Spectral fits to the ASCA and ROSAT X-ray spectra with absorbed power-law models in the mid and high energy bands result in spectral indices of  $1.93^{+0.27}_{-0.28}$  and  $2.01^{+0.1}_{-0.1}$  respectively. For the spectral model we assumed Galactic absorption with  $N_H = 4.47 \times 10^{20} \text{ cm}^{-2}$ .

#### 4.4. The Variable GL BAL Quasar PG1115+080

Recent observations of PG1115+080 in the FAR - UV with IUE (Michalitsianos et al. 1996) suggest the presence of a variable BAL region. In particular OVI $\lambda$  1033 emission and BAL absorption with peak outflow velocities of  $\sim 6,000 \text{ km s}^{-1}$  were observed to vary over timescales of weeks down to about 1 day. Variations in the BAL absorption features may be

due to changes in the ionization state of the BAL material that could lead to changes in the column density. A model proposed by Barlow et al. (1992) to explain the 1 day fluctuations considers the propagation of an ionization front in the BAL flow. We expect variations in the BAL column densities to also manifest themselves as large variations in the observed X-ray flux. We searched the HEASARC archives and found that PG1115+080 was observed with the Einstein IPC on Dec 5 1979, the ROSAT PSPC on Nov 21, 1991 and with the ROSAT HRI on May 27 1994. Using the XIMAGE tool *detect* on the ROSAT HRI and PSPC images of the PG1115+080 observations and searching the NED database we found several X-ray sources within a 15 arcmin radius of PG1115+080. Most of these sources were detected in the ROSAT International X-ray Optical Survey (RIXOS). A list of their coordinates and NED identifications is shown in Table 7. The source extraction regions used in the analysis of the PG1115+080 event files were circles centered on PG1115+080 with radii of 1.5 arcmin and 4 arcmin for the PSPC and Einstein observations of PG1115+080, respectively. We excluded regions containing the nearby RIXOS sources. The background regions were circles in the near vicinity of PG1115+080. We performed vari-

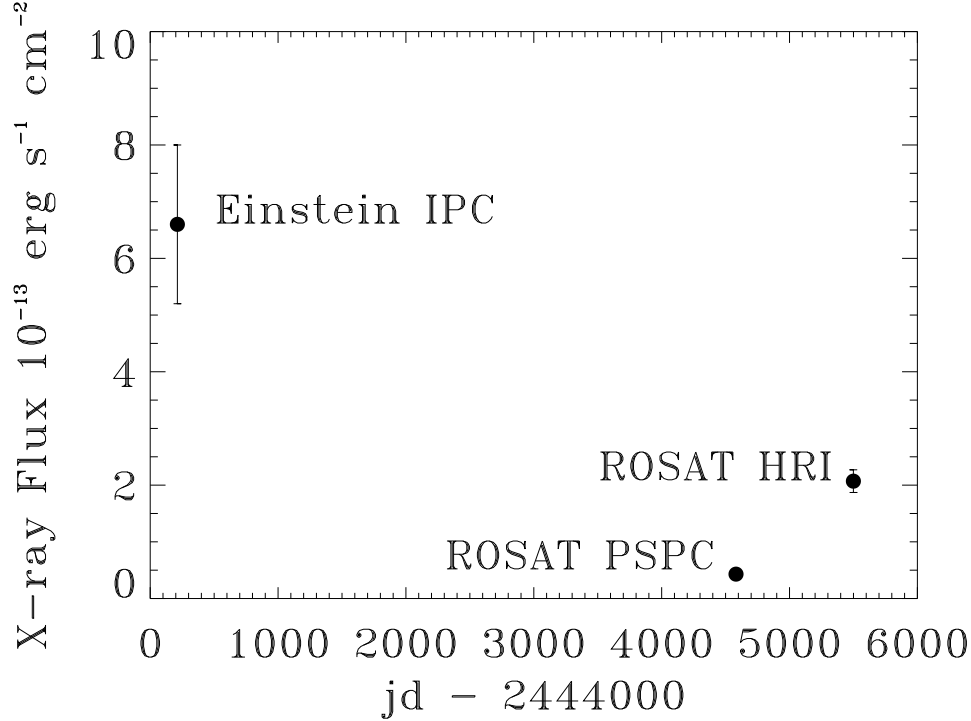


FIG. 6.— Estimated 0.2-2keV flux levels of PG1115+080 for the three available X-ray observations.

TABLE 5  
Model Parameters Determined from Spectral Fits to the  
*ASCA* SIS Spectra of B1422+231

Fit <sup>a</sup>	Date <sup>b</sup>	Instrument	$\alpha_{\nu 1}$	$\alpha_{\nu 2}$	Break Energy keV	$N_H(z=0)$ $10^{22} \text{ cm}^{-2}$	Flux 2-10 keV $10^{-12} \text{ erg s}^{-1} \text{ cm}^{-2}$	$\chi^2/(dof)$
1	t1	SIS0+	$1.55^{+0.08}_{-0.08}$			0.0252(fixed)	$1.70^{+0.46}_{-0.37}$	0.91(51)
	t1	SIS1					$1.58^{+0.43}_{-0.35}$	
2	t1	SIS0+	$2.06^{+0.42}_{-0.51}$	$1.51^{+0.08}_{-0.09}$	4.0	0.0252(fixed)	$1.74^{+0.27}_{-0.25}$	0.91(50)
	t1	SIS1					$1.64^{+0.26}_{-0.23}$	
3	t2	SIS0+	$1.46^{+0.1}_{-0.1}$			0.0252(fixed)	$2.02^{+0.73}_{-0.55}$	1.07(27)
	t2	SIS1					$1.92^{+0.69}_{-0.51}$	
4	t2	SIS0+	$0.3^{+1.4}_{-1.37}$	$1.52^{+0.12}_{-0.12}$	4.0	0.0252(fixed)	$1.93^{+0.40}_{-0.35}$	1.07(26)
	t2	SIS1					$1.84^{+0.39}_{-0.33}$	

NOTES-

<sup>a</sup> Fits 1 and 3 incorporate a redshifted power-law plus absorption due to cold material at solar abundances fixed to the Galactic value. Fit 2 and 4 incorporate a broken power-law with a break energy fixed at 4keV (rest frame) and absorption due to cold material at solar abundances fixed to the Galactic value. <sup>b</sup> t1 and t2 correspond to the observation dates of Jan 14, 1995 and July 17, 1995 respectively.

ous spectral fits to the PG1115+080 data with results summarized in Table 8. The observed Einstein IPC and ROSAT PSPC spectra of PG1115+080 accompanied by best fit models are shown in Figure 5. The X-ray observations of PG1115+080 with the ROSAT HRI show that all the detected X-ray emission is localized within a few arcsecs. We therefore do not expect any contamination from possible extended

lenses. The HRI image of the field near PG1115+080 is shown in Figure 9.

We modeled the observed spectra as power-laws with Galactic and intrinsic absorption. Our spectral fits to the Nov 21, 1991 observation imply absorption in excess to Galactic with a modeled intrinsic absorption of  $1.43^{+1.3}_{-1.3} \times 10^{22} \text{ cm}^{-2}$  assuming a power-law photon index of 2.3 appropriate for high redshift

TABLE 6  
Model Parameters Determined from Spectral Fits to the  
ROSAT PSPC and ASCA Spectra of HE1104-1805

Fit <sup>a</sup>	Instrument	$\alpha_\nu$	$N_H(z=0)$	Absorption Energy	Flux 2-10keV	$\chi^2/(dof)$
			$10^{22} \text{ cm}^{-2}$	keV	$10^{-13} \text{ erg s}^{-1} \text{ cm}^{-2}$	
1	SIS0+	$1.91^{+0.06}_{-0.06}$	0.0447(fixed)		$9.4^{+1.5}_{-1.4}$	1.19(98)
	SIS1				$8.3^{+1.4}_{-1.2}$	
2	ROSAT PSPC	$2.05^{+0.19}_{-0.21}$	0.0447(fixed)		$27.3^{+21.0}_{-10.6}$	1.14(17)

NOTES-

<sup>a</sup> Fit 1 incorporates a redshifted power-law plus absorption due to cold material at solar abundances fixed to the Galactic value.

TABLE 7  
Properties of Sources in the Near Vicinity of PG1115+080

Object	RA (J2000)	DEC (J2000)	z	Distance <sup>a</sup> arcmin	Count Rate <sup>b</sup> $10^{-3} \text{ cnts s}^{-1}$
RIXOS F258-032	11h18m22.1s	+07d44m49s	1.615	1.7	$3.93^{+0.64}_{-0.64}$
RIXOS F258-030	11h18m32.9s	+07d49m02s	0.847	5.0	$3.03^{+0.58}_{-0.58}$
RIXOS F258-001	11h17m50.7s	+07d57m12s	0.698	12.9	$14.9^{+1.3}_{-1.3}$
RIXOS F258-005	11h17m25.4s	+07d53m28s	0.811	14.8	$3.13^{+0.82}_{-0.82}$
CGCG 039-121	11h19m41.4s	+07d35m34s		23.4	$48.2^{+2.5}_{-2.5}$

NOTES-

<sup>a</sup> Distance from image PG1115+080 A.

<sup>b</sup> Count rates extracted from the Nov 1991 ROSAT PSPC observation of PG1115+080.

radio-quiet quasars (Fiore et al. 1998; Yuan et al. 1998). For photon indices ranging between 2 and 2.6 the best fit values for the intrinsic absorption ranges between 0.2 and  $3.5 \times 10^{22} \text{ cm}^{-2}$ .

To evaluate the statistical significance of the existence of intrinsic absorption we calculated the F statistic formed by taking the ratio of the difference of  $\chi^2$  between a fit with only Galactic absorption (fit 3 in Table 8) and a new fit that in addition to Galactic assumes intrinsic absorption (fit 4 in Table 8) to the reduced  $\chi^2$  of the new fit. We find an F value of 21 between fits 3 and 4 (see Table 8) implying that the addition of an intrinsic absorption component improves the fit to the Nov 21 1991 observation of PG1115+080 with a probability of exceeding F by chance of about 0.005. Our spectral fits to the Dec 5 1979 observations do not indicate absorption in excess to the Galactic one. In contrast to the Nov 21 1991 observation of PG1115+080, the inclusion of intrinsic absorption into our model for spectral fits to the Dec 5 1979 observation produces a significantly larger reduced  $\chi^2$ . The best fit value for the intrinsic absorber column for the Nov 21 1991 observation (fit 2, Table 8) is poorly constrained to be  $1.2^{+1.1}_{-1.1} \times$

$10^{23} \text{ cm}^{-2}$ . Notice however from Table 8 that this is a very model dependent result.

Our spectral model fits to the presently available X-ray observations of PG1115+080 indicate a decrease of about a factor of 13 of the 0.2-2keV flux between Dec 5 1979 and Nov 21 1991 and an increase by a factor of about 5 between the Nov 21 1991 and May 27 1994 observations. Figure 6 shows the estimated 0.2-2keV flux levels of PG1115+080 for the three X-ray observations.

The poor S/N of the available spectra make it difficult to discern the cause of the X-ray flux variability. Possible origins may include a change in the column density of the BAL absorber, intrinsic variability of the quasar or a combination of both these effects.

#### 4.5. Q1208+1011, Q1413+117, QJ0240-343

Q1208+1011 was observed with the ROSAT PSPC on Dec 16 1991 and June 3 1992, for 2,786 sec and 2,999 sec respectively. These short observations provide a weak constraint of  $2.66^{+2.1}_{-0.91}$  on the mid band 1-4 keV rest-frame photon index. The magnification factor of this lens system is estimated to be approximately 4, assuming a singular isothermal sphere lens potential and a lens redshift of  $z=1.1349$  (Siemigi-

TABLE 8  
Model Parameters Determined from Spectral Fits to the  
ROSAT PSPC and Einstein IPC Spectra of PG1115+080

Fit	Model <sup>a</sup>	Instruments <sup>b</sup>	$\alpha_\nu$	$N_H(z=0)$ $10^{22} \text{ cm}^{-2}$	$N_H(z=1.72)$ $10^{22} \text{ cm}^{-2}$	Flux 0.2-2keV $10^{-13} \text{ erg s}^{-1} \text{ cm}^{-2}$	$\chi^2/(dof)$
1	1	ROSAT PSPC	$1.38^{+0.15}_{-0.94}$	0.0368(fixed)	0	$0.52^{+0.06}_{-0.04}$	0.64(5)
2	2	ROSAT PSPC	$6.9^{+6.0}_{-6.0}$	0.0368(fixed)	$11.61^{+10.9}_{-10.6}$	<sup>c</sup>	0.27(4)
3	3	ROSAT PSPC	2.3(fixed)	0.0368(fixed)	0	$0.52^{+0.9}_{-0.9}$	1.66(6)
4	4	ROSAT PSPC	2.3(fixed)	0.0368(fixed)	$1.43^{+1.3}_{-1.3}$	$0.43^{+0.06}_{-0.05}$	0.39(5)
5	1	Einstein IPC	$2.05^{+0.86}_{-0.77}$	0.0368(fixed)	0	$6.03^{+2.02}_{-1.52}$	0.61(4)
6	3	Einstein IPC	2.3(fixed)	0.0368(fixed)	0	$6.60^{+1.4}_{-1.4}$	0.51(5)
7	4	Einstein IPC	2.3(fixed)	0.0368(fixed)	$0.4^{+2.4}_{-0.4}$	$5.50^{+1.06}_{-1.31}$	0.62(4)
8	5	ROSAT PSPC	2.3(fixed)	0.0368(fixed)	$1.43^{+1.2}_{-1.2}$	$0.43^{+0.13}_{-0.11}$	0.45(10)
		+Einstein IPC		0.0368(fixed)	0	$6.60^{+1.4}_{-1.4}$	
9	3	ROSAT PSPC	2.3(fixed)	0.0368(fixed)	0	$0.49^{+0.09}_{-0.09}$	1.14(11)
		+Einstein IPC		0.0368(fixed)	0	$6.60^{+1.4}_{-1.4}$	
10	4	ROSAT HRI	2.3(fixed)	0.0368(fixed)	0	$2.07^{+0.2}_{-0.2}$	

NOTES-

<sup>a</sup> Model 1 incorporates a redshifted power-law plus absorption due to cold material at solar abundances fixed to the Galactic value. Model 2 incorporates a redshifted power-law, absorption due to cold material at solar abundances fixed to the Galactic value and absorption due to cold material at solar abundances located a  $z=1.72$ . Model 3 incorporates a redshifted power-law with a photon index fixed at 2.3 plus absorption due to cold material at solar abundances fixed to the Galactic value. Model 4 incorporates a redshifted power-law with a photon index fixed at 2.3, absorption due to cold material at solar abundances fixed to the Galactic value and absorption due to cold material at solar abundances located a  $z=1.72$ . Model 5 models the ROSAT PSPC data as described in model 4 and models the Einstein PSPC data as described in model 3. <sup>b</sup> The ROSAT PSPC observation of PG1115+080 was made on Nov 21, 1991, the Einstein IPC on Dec 5 1979, and the ROSAT HRI on May 27 1994. <sup>c</sup> The X-ray flux is not well constrained in this fit.

TABLE 9  
Optical and X-ray<sup>b</sup> Properties of GL BAL Quasars

Object	z	m <sup>a</sup>	Outflow Velocity $\text{km s}^{-1}$	$L_X^b$ $10^{45} \text{ erg s}^{-1} \text{ keV}^{-1}$
PG1115+080	1.72	15.8(R)	6,000(O VI)	4.1
RXJ0911.4+0551	2.80	18.0(R)	3,200(C IV)	2.3
Q1120+0195	1.46	16.2(V)	12,000(O VI)	2.7
Q1413+117	2.55	17.0(R)	8,500(C IV)	3.9
APM08279+5255	3.87	15.2(R)	8,000(C IV)	37.1
HE2149-2745	2.03	16.5(R)	8,000(N V)	3.5
SBSG 1520+530	1.86	18.2(V)	20,000(C IV)	1.0

NOTES-

<sup>a</sup> Apparent optical magnitude of brightest image.

<sup>b</sup> The X-ray monochromatic luminosities are estimated at 2keV for the case of no absorption and with no correction due to the GL magnification effect. The X-ray luminosity estimate is based on the mean  $\alpha_{ox}$  for quasars derived by Green et al. 1995, and optical continuum luminosities were derived from the observed apparent magnitudes using the formulae described in Zamorani et al. (1981).

nowska et al. 1998). A recent application of the proximity effect, however, measured in the Lyman absorption spectrum of Q1208+1011 (Giallongo et al. 1998) implies an amplification factor as large as 22.

Q1413+117 is a BAL GL quasar observed with the ROSAT PSPC on July 20, 1991 for 27,863sec. Using the standard detect and spectral fitting software tools

XIMAGE-SOSTA, XIMAGE-detect and XSELECT-XSPEC we detect Q1413+117 at the  $3\sigma$  level in the ROSAT PSPC observation. The ROSAT PSPC and optical (HST) source coordinates of Q1413+117 are 14h 15m 46.4s,  $+11^\circ 29' 56.3''$  (J2000), and 14h 15m 45s,  $+11^\circ 29' 42''$  (J2000) respectively. The ROSAT and HST positions are well within the uncertainty of

the ROSAT PSPC pointing accuracy. The improvements made in the processing of the ROSAT raw data by the U.S. ROSAT Science Data Center from the revision 0 product (rp700122) to the revision 2 product (rp700122n00), used in this analysis, may explain the non-detection of Q1413+117 in the Green & Mathur 1995 paper.

We fitted the poor S/N PSPC spectrum of Q1413+117 with a power-law model that included Galactic and intrinsic absorption due to cold gas at solar abundances. For photon indices ranging between 2.0 and 2.6 our spectral fits imply intrinsic column densities ranging between 2 and  $14 \times 10^{22} \text{ cm}^{-2}$ .

Recently a pair of bright UV-excess objects, QJ0240-343 A and B, with a separation of  $6.1''$  were discovered by Tinney (1997). The redshift of both objects was found to be 1.4, while no lens has been detected. Monitoring of this system in the optical indicates that it is variable on timescales of a few years. Spectra taken with the 3.9m Anglo-Australian telescope show a metal-line absorption system at  $z = 0.543$  and a possible system at  $z = 0.337$ . QJ0240-343 was observed with the ROSAT PSPC in January 1992 with a detected count rate of  $2.9 \pm 0.7 \times 10^{-3} \text{ cts s}^{-1}$ . GL theory predicts that the lens for this system lies at about  $z = 0.5$ . The geometry of this system is very similar to that of the double lens Q0957+561. The large angular image separation of the proposed GL system QJ0240-343 suggests the presence of a lens consisting of a galaxy cluster. The lens however has yet to be detected and it has been suggested that this may be a binary quasar system.

## 5. DISCUSSION

### 5.1. X-ray Properties of Faint Quasars

Our present sample of moderate to high S/N ASCA and ROSAT X-ray spectra of GL quasars contains two radio-loud quasars, Q0957+561 and B1422+231 (see Figures 1 and 2), and three radio-quiet quasars, HE1104-1805 (see Figure 3), SBS0909+532 (see figure 4) and Q1208+1011. Derived photon indices in the soft, mid and hard bands for these objects are presented in Table 2. For the two radio-loud quasars Q0957+561 and B1422+231 we observe a flattening of the spectra between mid and hard bands while for the radio-quiet quasar HE1104-1805 we do not observe any significant change in spectral slope between mid and hard bands. The spectral flattening of radio-loud quasars between mid and hard energy bands has been reported for non-lensed quasars (e.g. Wilkes & Elvis 1987; Fiore et al. 1998; Laor et al. 1997). The present findings for GL quasars are consistent with those for non-lensed quasars and imply that the underlying mechanism responsible for the

spectral hardening in the hard band persists for the relatively high redshift GL quasars of our sample with X-ray luminosities that are less (by magnification factors ranging between 2 and 30) than previously observed objects at similar redshifts.

Our analysis makes use of the GL amplification effect to extend the study of quasar properties to X-ray flux levels as low as a few  $\times 10^{-16} \text{ erg s}^{-1} \text{ cm}^{-2}$ . The limiting sensitivity of the ROSAT All-sky Survey, for example, on which many recent studies are based, is a few  $\times 10^{-13} \text{ erg s}^{-1} \text{ cm}^{-2}$ . We find that the spectral slopes of the radio-loud and non BAL quiet-quasars of our sample are consistent with those found in quasars of higher flux levels and do not appear to approach the observed spectral index of  $\sim 1.4$  of the hard X-ray background. Absorption due to known intervening systems in Q0957+561, B1422+231, SBS0909+532, Q1208+1011 and HE1104-1805 apparently does not lead to the spectral hardening observed in the Vikhlinin et al. (1995) sample at flux levels below  $\sim 10^{-13} \text{ erg s}^{-1} \text{ cm}^{-2}$ . However, we do find that modeling the two radio-quiet BAL quasars PG1115+080 and Q1413+117 and the radio-loud quasar PKS1830-211, which shows strong X-ray absorption (Mathur et al. 1997), with simple power-law models with Galactic absorption results in very low spectral indices (see Table 2). Similar unlensed sources will therefore contribute to the remaining unresolved portion of the XRB. The presently available sample size of X-ray detected BAL radio-quiet quasars, however, will have to be significantly increased before we can make a statistically significant quantitative assessment of the BAL quasar contribution to the hard XRB.

### 5.2. X-ray Properties of Gravitationally Lensed BAL Quasars

Approximately 10% of optically selected quasars have optical/UV spectra that show deep, high-velocity Broad Absorption Lines (BAL) due mostly to highly ionized species such as C IV, Si IV, N V and O VI. However, a small fraction of BAL quasars show low ionization transitions of Mg II, Al III, Fe II and Fe III as well (e.g. Wampler et al. 1995). The observed absorption troughs are found bluewards of the associated resonance lines and are attributed (see Turnshek et al. 1988) to highly ionized gas flowing away from the central source at speeds ranging between 5,000 and 30,000  $\text{km s}^{-1}$ . Recent polarization observations (Goodrich 1997) indicate that the true fraction of BAL's and BAL covering factors may be substantially larger ( $> 30\%$ ) than the presently quoted value of 10%. Only a very small number of BAL quasars and AGN have been reported in the literature with detections in the X-ray band (PHL5200, Mrk231, SBS1542+541, 1246-057, and Q1120+0195(UM425)).

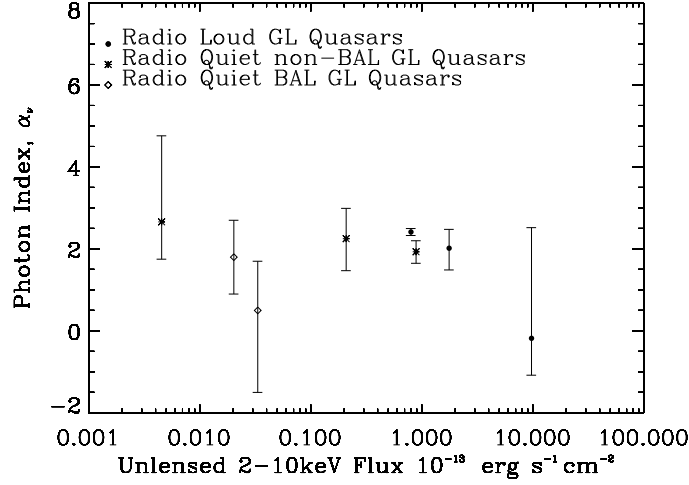


FIG. 7.— Photons indices for radio-loud and radio-quiet GL quasars of our sample as a function of the unlensed 2-10keV flux.

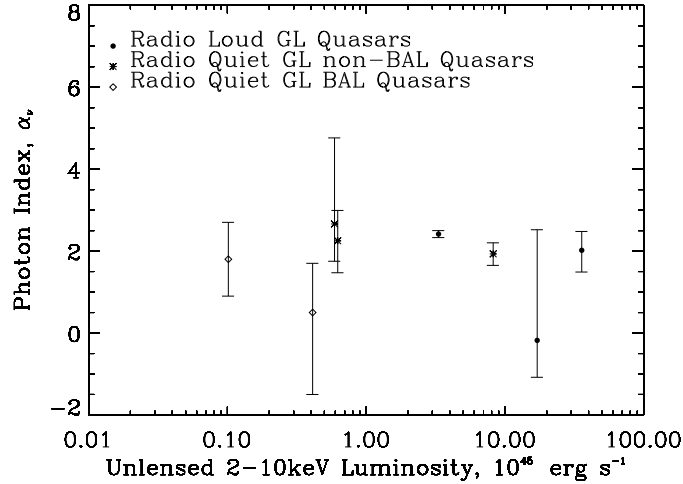


FIG. 8.— Photons indices for radio-loud and radio-quiet GL quasars of our sample as a function of the 2-10keV luminosity. X-ray luminosities have been corrected for the magnification effect.

With this work we also add to the list of X-ray detected BAL quasars the GL quasars PG1115+080, Q1413+117 and possibly RXJ0911.4+0551. We consider PG1115+080 and RXJ0911.4+0551 intermediate BAL quasars because of the relatively low peak velocities of the outflowing absorbers (see Table 9 for a list of outflowing velocities of GL BAL quasars). The X-ray spectra obtained from X-ray observations of BAL quasars have modest (PHL5200, & Mrk231) to

poor S/N and cannot accurately constrain the BAL column densities.

Several of the GL quasars of our sample are known to contain intervening and intrinsic absorption. In particular PG1115+080 is known to contain a variable BAL system (Michalitsianos et al. 1996). The available X-ray observations indicate that PG1115+080 is a highly variable X-ray source. The large X-ray flux variations (a factor of about 13 de-

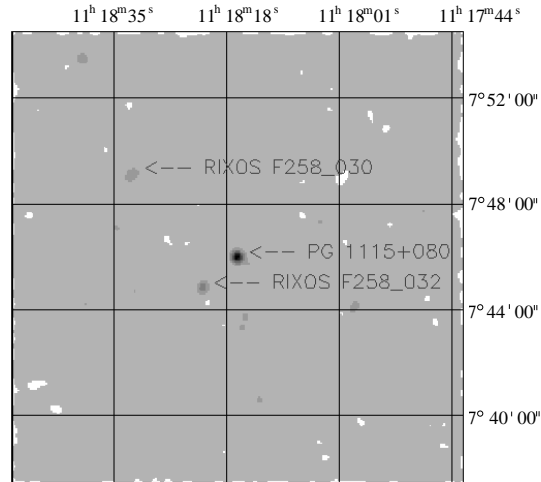


FIG. 9.— HRI image of the field near PG1115+080.

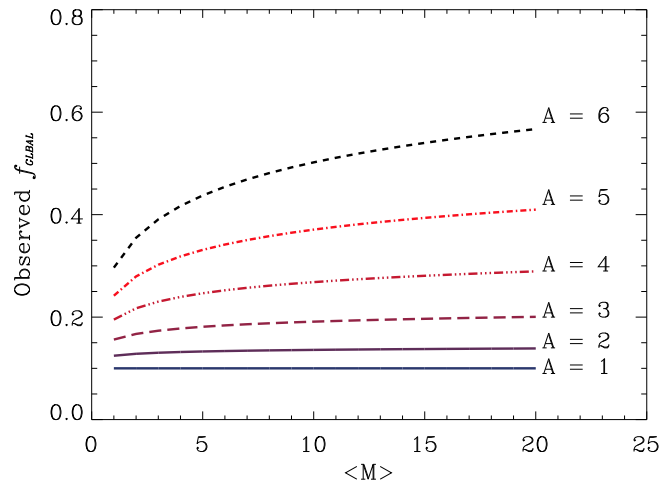


FIG. 10.— Plot of the estimated observed fraction of GL BAL quasars as a function of attenuation value  $A$  and magnification factor  $\langle M \rangle$ .

crease in X-ray flux between December 5 1979 and November 21 1991 and about a factor of 5 increase between November 21 1991 and May 27 1994) may possibly be used to substantially reduce the errors in the determination of the time delay of this GL system. Such a monitoring program will have to await the launch of the Chandra X-ray Observatory (CXO), a.k.a. AXAF, which has the spatial resolution to resolve the lensed images.

The GL quasars Q1413+117, Q1120+0195 and

RXJ0911.4+0551 have also been detected in X-rays and are known to contain BAL features. Unfortunately the available X-ray data have poor S/N and we have only provided estimates of their X-ray flux and luminosity. Recent high resolution optical and NIR imaging of RXJ0911.4+0551 have resolved the object into four lensed images and a lensing galaxy (Burud et al. 1998). They also detect a candidate galaxy cluster  $38''$  away from the image A1 with an estimated redshift of 0.7. It is possible that a large



fraction of the detected X-ray emission in the ROSAT HRI observations of RXJ0911.4+0551 is originating from the cluster of galaxies.

An interesting finding made by searching through the literature is the apparently large fraction of optically detected GL BAL quasars. In particular we found seven GL BAL quasars out of a total of about 20 radio-quiet GL quasar candidates known to date. The probability of finding 7 or more BAL quasars out of a sample of 20 GL radio-quiet quasars assuming a true BAL fraction (amongst radio-quiet quasars only) of 0.11 is about  $4 \times 10^{-3}$ . In Table 9 we list several properties of these GL BAL quasars. Thus we find that at least 35% of radio-quiet gravitationally lensed quasars contain BAL features which is significantly larger than the 10% fraction of BAL quasars found in optically selected quasar samples (almost all BAL's are radio-quiet and about 90% of optically selected quasars are radio-quiet). Recently, BAL's have also been identified in a few radio-loud quasars (Brotherton et al. 1998). These observations suggest that a large fraction of BAL quasars are missed from flux limited optical surveys, a view that has also been proposed by Goodrich (1997) based on polarization measurements of BAL quasars. One plausible explanation for the over-abundance of BAL quasars amongst radio-quiet GL quasars is based on the GL magnification effect which causes the luminosity distributions of BAL quasars and GL BAL quasars to differ considerably such that presently available flux limited surveys of BAL quasars detect more GL BAL quasars. We have created a simple model that can explain the difference between the observed GL BAL fraction of  $\sim 35\%$  and the observed non-lensed BAL quasar fraction of  $\sim 10\%$ .

Our model makes use of the quasar luminosity function as parameterized by Pei (1995), assumes that only 20% of BALs observed in optical surveys of unlensed quasars are attenuated by a factor A (see Goodrich, 1997) and it uses the Warren et al. (1994) optical limits for non-lensed quasars and the CASTLES survey optical limits for lensed quasars (Kochanek et al. 1998). To simplify the analysis we assume an average magnification factor of  $\langle M \rangle$  for the GL quasars rather than incorporate each magnification factor separately.

A survey of lensed quasars, with luminosity limits between  $L_1$  and  $L_2$ , will have a *true* luminosity range, assuming an average lens magnification factor of  $\langle M \rangle$ , that lies between  $\frac{L_1}{\langle M \rangle}$  and  $\frac{L_2}{\langle M \rangle}$  for unattenuated lensed BAL quasars and that lies between  $\frac{L_1 A}{\langle M \rangle}$  and  $\frac{L_2 A}{\langle M \rangle}$  for attenuated lensed BAL quasars. Following the arguments of Goodrich (1997) we assume that only an observed fraction of 20% of BAL quasars are attenuated (this is approximately the ob-

served fraction of BAL quasars with significant polarization). Based on what we have just discussed, the observed fraction,  $f_{ogb}(L_1, L_2)$ , of GL BAL quasars in the luminosity range of  $L_1$  to  $L_2$  can be approximated with the observed fraction,  $f_{ob}(\frac{L_1}{\langle M \rangle}, \frac{L_2}{\langle M \rangle})$ , of non-GL BAL quasars in the *observed* luminosity range of  $\frac{L_1}{\langle M \rangle}$  to  $\frac{L_2}{\langle M \rangle}$ .

$$f_{ogb}(L_1, L_2) = f_{ob}(\frac{L_1}{\langle M \rangle}, \frac{L_2}{\langle M \rangle}) \quad (4)$$

We separate the observed BAL quasar fraction,  $f_{ob}(\frac{L_1}{\langle M \rangle}, \frac{L_2}{\langle M \rangle})$ , into the fraction that is attenuated,  $f_{oba}(\frac{L_1}{\langle M \rangle}, \frac{L_2}{\langle M \rangle})$ , and the fraction  $f_{obna}(\frac{L_1}{\langle M \rangle}, \frac{L_2}{\langle M \rangle})$  that is not attenuated,

$$\begin{aligned} f_{ob}(\frac{L_1}{\langle M \rangle}, \frac{L_2}{\langle M \rangle}) = \\ f_{oba}(\frac{L_1}{\langle M \rangle}, \frac{L_2}{\langle M \rangle}) + \\ f_{obna}(\frac{L_1}{\langle M \rangle}, \frac{L_2}{\langle M \rangle}) \end{aligned} \quad (5)$$

If we assume that the luminosity distribution of non-attenuated BAL quasars is similar to that of non BAL quasars we expect the fraction  $f_{obna}(\frac{L_1}{\langle M \rangle}, \frac{L_2}{\langle M \rangle})$  to be independent of luminosity range and therefore approximately equal to the observed value  $f_{obna}(L_3, L_4) \sim 8\%$ , where  $L_3$  and  $L_4$  are the Warren et al. (1994) optical luminosity limits.

As pointed out by Goodrich 1997 the attenuation expected to be present in about 20% of all BAL quasars causes the observed luminosity function for BAL quasars to be considerably different from the true luminosity function for BAL quasars.

The ratio of observed,  $f_{oba}$ , to true,  $f_{tba}$ , fraction of attenuated BAL quasars can be determined if one incorporates the effect of attenuation in the quasar luminosity function. In particular if we define  $N(\frac{L_1}{\langle M \rangle}, \frac{L_2}{\langle M \rangle}, z_1, z_2)$  as the integral of the quasar luminosity function as parametrized by Pei (1995) over the luminosity range  $\frac{L_1}{\langle M \rangle}$  and  $\frac{L_2}{\langle M \rangle}$  and the redshift range  $z_1$  and  $z_2$  then we may write the ratio of observed to true fraction of attenuated BAL quasars within this luminosity range as,

$$\frac{f_{oba}(\frac{L_1}{\langle M \rangle}, \frac{L_2}{\langle M \rangle})}{f_{tba}} = \frac{N(\frac{L_1 A}{\langle M \rangle}, \frac{L_2 A}{\langle M \rangle}, z_1, z_2)}{N(\frac{L_1}{\langle M \rangle}, \frac{L_2}{\langle M \rangle}, z_1, z_2)} \quad (6)$$

The observed fraction of about 2% of attenuated non-lensed BAL quasars, however, is measured within the Warren et al. (1994) optical limits of  $L_3 = 2.7 \times 10^{46}$  erg s $^{-1}$  and  $L_4 = 3.8 \times 10^{47}$  erg s $^{-1}$  and redshift range of  $z_3 = 2$  and  $z_4 = 4.5$ . We therefore write the ratio of observed to true fraction of attenuated BAL quasars within the  $L_3$  and  $L_4$  range as,

$$\frac{f_{oba}(L_3, L_4)}{f_{tba}} = \frac{N(L_3 A, L_4 A, z_3, z_4)}{N(L_3, L_4, z_3, z_4)} \quad (7)$$

Combining equations 4, 5, 6 and 7 we obtain the following expression for the observed fraction of GL BAL quasars as a function of average GL magnification  $\langle M \rangle$  and BAL attenuation factor  $A$ ,

$$f_{ogb}(L_1, L_2) = f_{obna}(L_3, L_4) + f_{oba}(L_3, L_4) \times \frac{N(L_3, L_4, z_3, z_4)}{N(L_3 A, L_4 A, z_3, z_4)} \frac{N(\frac{L_1 A}{\langle M \rangle}, \frac{L_2 A}{\langle M \rangle}, z_1, z_2)}{N(\frac{L_1}{\langle M \rangle}, \frac{L_2}{\langle M \rangle}, z_1, z_2)} \quad (8)$$

In Figure 10 we plot the expected observed fraction of GL BAL quasars as a function of attenuation values  $A$  and magnification factors  $\langle M \rangle$ .

The magnification effect of GL quasars alone cannot explain the observed enhanced GL BAL quasar fraction of  $\sim 35\%$ . By combining, however, the magnification effect with the presence of an attenuation of the continuum in a fraction of BAL quasars, as suggested by the polarization observations by Goodrich 1997, our simple model can reproduce the observed GL BAL quasar fraction of  $\sim 35\%$ . For a range of average magnification factors  $\langle M \rangle$  between 5 and 15 we obtain attenuation values  $A$  ranging between 5 and 4.5. The range of attenuation values of 4.5 to 5, suggested by the observed fraction of GL BALQSO's, is close to the range of 3 to 4 implied by the observed polarization distributions of BALQSO's and non-BAL radio-quiet quasars (Goodrich 1997), especially considering the uncertainties in both analyses. A value of  $\langle M \rangle \sim 10$  is consistent with typical estimated values for GL quasars, (see, for example, our GL model estimates in Table 3).

## 6. CONCLUSIONS

We have introduced a new approach in studying the X-ray properties of faint quasars. Our analysis makes use of the GL amplification effect to extend the study of quasar properties to X-ray flux levels as low as a few  $\times 10^{-16}$  erg s $^{-1}$  cm $^{-2}$ . For the two radio-loud GL quasars Q0957+561 and B1422+231 we observe a flattening of the spectra between mid and hard bands (rest-frame) while for the radio-quiet quasar HE1104-1805 we do not observe any significant change in spectral slope between mid and hard bands. The present findings in GL quasars are consistent with those of non-lensed quasars and imply that the underlying mechanism responsible for the spectral hardening from mid to hard bands persists for the relatively high redshift GL radio-loud quasars of our sample with X-ray luminosities that are less (by the magnification factors indicated in Table 3) than previously observed objects at similar redshifts.

Our results suggest that radio-loud and non-BAL radio-quiet quasars with unlensed fluxes as low as a few  $\times 10^{-16}$  erg s $^{-1}$  cm $^{-2}$  do not have spectral slopes that are any different from brighter quasars. Modeling the spectra of the two GL BAL quasars and the radio-loud quasar PKS1830-211 in our sample with simple power-laws and including only Galactic absorption leads to spectral indices that are considerably flatter than the average values for quasars. These results therefore imply that BAL quasars and quasars with associated absorption will contribute to the unresolved portion of the hard XRB. We must emphasize, however, that our present sample of GL quasars will need to be enlarged to assess the significance of the contribution of BAL quasars to the XRB. X-ray observations in the near future with the X-ray missions CXO, XMM and ASTRO-E will significantly aid in adding many more GL quasars to this sample.

Our analysis of several X-ray observations of the GL BAL quasar PG1115+080 show that it is an extremely variable source. Fits of various models to the spectra obtained during these observations suggest that the X-ray variability is partly due to a variable BAL absorber. The X-ray flux variability in this source can be used to improve present measurements of the time delay. The large variability in the X-ray compared to optical band offers the prospect of substantially reducing the errors in deriving a time delay from cross-correlating image light curves. A precise measurement of the time delay combined with an accurate model for the mass distribution of the lens can be used to derive a Hubble constant that does not depend on the reliability of a "standard candle". The scheduled monitoring of PG1115+080 with the CXO will provide spatially resolved spectra and light curves for the individual lensed images.

One of the significant findings of this work was a surprisingly large fraction of BAL quasars that are gravitationally lensed. In particular we find 7 BAL quasars out of a sample of 20 GL radio-quiet quasars. We have successfully modeled this effect and find that an attenuation factor  $A \sim 5$  of the BAL continuum of only 20% of all BAL quasars is consistent with the observed GL fraction of 35%. We emphasize that the magnification effect alone cannot explain the observed difference between BAL fractions for lensed and non-lensed quasars. One needs to incorporate in addition an attenuation mechanism to produce the observed results. These observations therefore are suggestive of the existence of a hidden population of absorbed high redshift quasars which have eluded detection by present flux limited surveys. As X-ray and optical surveys approach lower flux limits we expect the fraction of BAL quasars found to increase.

I would like to thank N. Brandt, M. Eracleous, G. Garmire, and J. Nousek for helpful discussions and comments. This work was supported by NASA grant NAS 8-38252. This research has made use of data ob-

tained through the High Energy Astrophysics Science Archive Research Center Online Service, provided by the NASA/Goddard Space Flight Center.

## REFERENCES

- Angonin-Willaime, M. C., Hammer, F., & Rigaut, F., proceedings of the 31<sup>st</sup> Liege International Astrophysics Colloquium, Gravitational Lenses in the Universe, 1993
- Bade, N., Siebert, J., Lopez, S., Voges, W., & Reimers, D., 1997, *A&A*, 317, 13
- Barlow, T. A., Junkkarinen, Vesa, T., Burbidge, E. M., Weyman, R. J., Morris, S. L., & Korista, K. T., 1992, *ApJ*, 397, 81
- Bechtold, J., & Yee, H. K. C., 1995, *AJ*, 110, 1984
- Bechtold, J., Elvis, M., Fiore, F., Kuhn, O., Cutri, R. M., McDowell, J. C., Rieke, M., Siemiginowska, A., & Wilkes, B. J., 1994, *ApJ*, 108, 759.
- Brinkmann, W., Yuan, W., & Siebert, J., 1997, *A&A*, 319, 413
- Brotherton, M. S., Van Breugel, W., Smith, R. J., Boyle, B., J., Shanks, T., Croom, S. M., Miller, L., & Becker, R. H., 1998, *ApJ*, 505, L7
- Burud, I., Courbin, F., Lidman, C., Jaunsen, A. O., Hjorth, J., Ostensen, R., Andersen, M. I., Clasen, J. W., Wucknitz, O., Meylan, G., Magain, P., Stabell, R. and Refsdal, S., 1998, *ApJ*, 501, L5.
- Cappi, M., Matsuoka, M., Comastri, A., Brinkmann, W., Elvis, M., Palumbo, G. G. C., & Vignali, C., 1997, *ApJ*, 478, 492
- Chartas, G., Falco, E. E., Forman, W. R., Jones, C., Schild, R., & Shapiro, I. I., 1995, *ApJ*, 445, 140
- Chartas, G., Chuss, D., E., Forman, W. R., Jones, C., & Shapiro, I. I., 1998, *ApJ*, 504, 661
- Courbin, F., Lidman, C., & Magain, P., 1998, *A&A*, 330, 57
- Elvis, M., Fiore, F., Wilkes, B. J., McDowell, J. C., & Bechtold, J., 1994, *ApJ*, 422, 60
- Falco, E. E., Shapiro, I. I., Moustakas, L. A., & Davis, M., 1997, *ApJ*, 484, 70
- Fiore, F., Elvis, M., Giommi, P., & Padovani, P., 1998, *ApJ*, 492, 79
- Giallongo, E., Fontana, A., Cristiani, S., and D'Odorico S., 1999, *ApJ*, 510, 605
- Goodrich, R. W., 1997, *ApJ*, 474, 606
- Green, P. J., Schartel, N., Anderson, S. F., Hewett, P. C., Foltz, C. B., Brinkmann, W., Fink, H., Truemper, J., & Margon, B., 1995, *ApJ*, 450, 51
- Green, P. J., & Mathur, S., 1996, *ApJ*, 462, 637
- Inoue, H., Kii, T., Ogasaka, Y., Takahashi, T., & Ueda, Y. 1996, in *Proc. Int. Conf. on Röntgenstrahlung from the Universe*, ed. H. U. Zimmermann, J. Trümper, & H. Yorke (MPE Report 263; Garching: Max-Planck-Inst. Extraterr. Phys.) 323
- Keeton, C. R., Kochanek, C. S., & Falco, E. E., 1998, *ApJ*, 509, 561
- Kochanek, C. S., 1996, *ApJ*, 466, 638
- Kochanek, C. S., Falco, E. E., & Munoz, J. A., 1999, *ApJ*, 510, 590
- Kochanek, C. S., Falco, E. E., Schild, R., Dobrzycki, A., Engels, D., & Hagen, H., 1997, *ApJ*, 479, 678.
- Kochanek, C. S., Falco, E. E., Impey, C. D., Lehar, J., McLeod, B. A., & Rix, H.-W., 1998, *Proceedings of the 9th Annual Astrophysics Conference in Maryland, After the Dark Ages: When Galaxies Were Young*
- Kormann, R., Schneider, P., and Bartelmann, M., 1994, *A&A*, 286, 35
- Laor, A., Fiore, F., Elvis, M., Wilkes, B., & McDowell, J. C., 1997, *ApJ*, 477, 931
- Mathur, S., & Nair, S., 1997, *ApJ*, 484, 140
- Michalitsianos, A. G., & Oliversen, R. J., 1996, *ApJ*, 461, 593
- Nadeau, D., Yee, H. K. C., Forrest, W. J., Garnett, J. D., Ninkov, Z., & Pipher, J. L., 1991, *ApJ*, 376, 430
- Osoz, A., Serra-Ricart, M., Mediavilla, E., Buitrago, J., & Goicoechea, L., 1997, *ApJ*, 491, L7
- Patnaik, A., R., Browne, I. W. A., Walsh, D., Chafee, F. H., & Foltz, C. B., 1992, *MNRAS*, 259, 1
- Pei, Y. C., 1995, *ApJ*, 438, 623
- Reeves, J. N., Turner, M. J. L., Ohashi, T., & Kii, T., 1997, *MNRAS*, 292, 468
- Reimers, D., Bade, N., Schartel, N., Hagen, H., J., Engels, D., & Toussaint, F., 1995, *A&A*, 295, L49
- Siemiginowska, A., Bechtold, J., Aldcroft, T. L., McLeod, K. K., & Keeton, C. R., 1998, *ApJ*, 503, 118
- Schartel, N., Green, P., Anderson, S., Scott, F., Hewett, P. C., Foltz, C. B., Margon, B., Brinkmann, W., Fink, H., & Trumper, J., 1996, *MNRAS*, 283, 1015
- Smette, A., Gull, T. R. & Sahu, M. S., 1998, *AAS*, 193, 108.11
- Tinney, C. G., Da Costa, G. S., and Zinnecker, H., 1997, *MNRAS*, 285, 111
- Tonry, J. L., 1998, *AJ*, 115, 1
- Turnshek, D. A., Grillmair, C. J., Foltz, C. B., & Weymann, R. J., 1988, *ApJ*, 325, 651
- Ueda, Y. 1996, Ph.D. thesis, Univ. Tokyo
- Ueda, Y., et al. 1998, *Nature*, 391, 866
- Vikhlinin, A., Forman, W., Jones, C., & Murray, S., 1995, *ApJ*, 451, 564
- Wampler, E. J., Chugai, N. N., & Petitjean, P., 1995, *ApJ*, 443, 586
- Warren, S. J., Hewett, P. C., & Osmer, P., 1994, *ApJ*, 421, 412
- Wilkes, B., & Elvis, M., 1987, *ApJ*, 323, 243
- Yuan, W., Brinkmann, W., Siebert, J., & Voges, W., 1998, *A&A*, 330, 108
- Zamorani, G., Henry, J. P., Maccacaro, T., Tananbaum, H., Soltan, A., Avni, Y., Liebert, J., Stocke, J., Strittmatter, P. A., Weymann, R. J., Smith, M. G., & Condon, J. J., 1981, *ApJ*, 245, 357